Two-layer control structure for enhancing frequency stability of the MTDC system

Stojković, Jelena; Shetgaonkar, Ajay; Stefanov, Predrag; Lekić, Aleksandra

DOI
10.1016/j.ijepes.2022.108664

Publication date
2023

Document Version
Final published version

Published in
International Journal of Electrical Power and Energy Systems

Electrical Power and Energy Systems 145 (2023) 108664

Contents lists available at ScienceDirect

International Journal of Electrical Power and Energy Systems

journal homepage: www.elsevier.com/locate/ijepes

Two-layer control structure for enhancing frequency stability of the MTDC system

Jelena Stojković [a,*], Ajay Shetgaonkar [b], Predrag Stefanov [a], Aleksandra Lekić [b]

[a] School of Electrical Engineering, University of Belgrade, Belgrade, Serbia
[b] Intelligent Electrical Power Grids (IEPG-ESE), TU Delft, Delft, The Netherlands

ARTICLE INFO

Keywords:
Adaptive droop control
Frequency control
Multi-terminal DC grids
Power sharing

ABSTRACT

This paper explores the possibilities of providing fast frequency support as an emergency support service to the disturbed AC system through the MTDC grid. A two-layer hierarchical control structure of the MTDC grid is proposed to assure the minimum cost of the frequency control actions, the minimum voltage deviations, or the minimal impact on the frequencies of not-affected AC systems while ensuring the stable operation of MTDC grid. An optimization algorithm is executed at the secondary control level to find the optimal reference values for the voltage-droop characteristics of the voltage-regulating converters, and consequently their DC voltages and active power references. Then, at the primary control level, the reference values are tuned with the optimization results. Implemented control structure confirms that MTDC can provide set values at its terminals without endangering its stability. The secondary control layer is implemented in MATLAB, while the performance of the controller is successfully evaluated through simulation in RSCAD.

1. Introduction

The rising penetration of the converter-interfaced renewable energy sources (RES) is causing a decrease in rotation inertia, and it is consequently threatening the quality of the traditional frequency control [1]. On the other hand, multi-terminal dc (MTDC) systems are widely used for the integration of RES and have the capability to change the active power fast. Because of their flexibility, MTDC systems are seen as a valuable resource that can provide fast frequency response (FFR) in low-inertia grids [2,3]. Although AC systems connected through the MTDC grid are independent in terms of frequency stability, they can share power reserves and provide frequency support to another AC system after a frequency disturbance. Therefore, the burden of the frequency support will be shared by the AC grids that can provide this kind of service connected via MTDC system.

Common control strategies for the MTDC system include master–slave control (MSC) [4], voltage margin strategy [5], and DC voltage droop control strategies [6–14]. The general disadvantage of MSC-based control strategies lays in the fact that the MTDC system will be paralyzed once the master converter stops working. The voltage margin method, which can be seen as an extension of MSC, experiences oscillations in DC voltages when the master converter is shifted. Contrary to MSC and voltage margin control, that are centralized and therefore rely on the fast and reliable communication system, droop control has distributed nature, and communication delays that may affect the controller performance are avoided. Droop-based control is scalable and easily implemented and therefore, it is adopted in this paper.

Autonomous power-sharing and frequency support through power droop-controlled converters in MTDC systems have been a recent topic for research. The control strategy in [6] enables mutual frequency support among AC networks in the MTDC considering the frequency variation perspective of the AC network, while authors in [7] propose a decoupled frequency control scheme to improve weak AC systems frequency stability. In [8] authors propose distributed control structure for sharing frequency containment that minimizes the generation costs and cost function related to deviations from the nominal DC voltages. However, control strategies in [6–8] do not consider constraints related to line capacities, although the perturbations from the operating point after a disturbance are not insignificant. The control strategy presented in this paper includes mentioned constraints and minimize the RoCoF values of AC systems that participate in power support. [9] proposes cost-based adaptive droop control strategy for frequency support in MTDC systems that shares the burden based on the available capacity of VSCs at the post-contingency-steady-state. However, authors focus on rectifier outage, not on frequency support in case of a disturbance in one of the AC systems. Adaptive droop control that ensures that DC voltage deviations are within their limits during

* Corresponding author.
E-mail address: jstojkovic@etf.bg.ac.rs (J. Stojković).

https://doi.org/10.1016/j.ijepes.2022.108664
Received 24 March 2022; Received in revised form 19 July 2022; Accepted 19 September 2022
Available online 13 October 2022

Nomenclature

Optimization definition

P_i^{res}	FFR reserve available in the AC system $i \in \{1,\dots,n_{AC}\}$
P_i^{sch}	scheduled power transmission value on the converter i
P^{sp}	power support of the disturbed AC system
P_i^{FFR}	FFR support from the AC system $i \in \{1,\dots,n_{AC}\}$ in case of disturbance in AC system $j \in \{1,\dots,n_{AC}\}$, $j \neq i$
P_j^{DC}	power flow of the DC line $j \in \{1,\dots,n_{DC}\}$
P_i^{cap}	capacity of converter $i \in \{1,\dots,n_{MMC}\}$
$c_i^{FFR}(\cdot)$	cost of FFR reserve in the AC system $i \in \{1,\dots,n_{AC}\}$
$\min F$	optimization problem
$RoCoF$	rate of changing of frequency
U_i^{DC}	DC side voltage of the converter $i \in \{1,\dots,n_{MMC}\}$
$G_{i,j}$	conductance at the position (i,j) of the network admittance matrix
ΔU_i	change in DC voltage of the converter $i \in \{1,\dots,n_{MMC}\}$
ΔP_i	change in active power of the converter $i \in \{1,\dots,n_{MMC}\}$
k_i	voltage-droop coefficient of the ith converter, $i \in \{1,\dots,n_{MMC}\}$
n_{AC}	number of AC systems interconnected through the MTDC grid
n_{DC}	number of DC lines
N_{dist}	number of potential disturbances in specific AC system
$i_{current\_dist}$	number of the current disturbance from the defined list, $i_{current\_dist} \in \{1,\dots,N_{dist}\}$

MMC's parameters

v_{AC}	AC side voltage
i_{AC}	AC side current
v_{DC}	DC side voltage
P	active AC power
P_{ref}	reference value of the active AC power
Q	reactive AC power
k_{droop}	droop coefficient

Standard definitions

ref	reference value
rms	root mean square value
max	maximum value
min	minimum value
PI	proportional integral controller
PLL	phase locked loop

large disturbances is proposed in [10,11], but the impact of varying droop coefficients on the stability of the MTDC system has not been elaborated. Contrary to this approach, we present a method where the droop coefficient does not change continuously, and it is adapted only two times after a disturbance happened which is favorable in terms of control complexity and system stability. The adaptive droop control strategy proposed in [12] effectively shares the power between terminals in the MTDC grid and controls DC voltage deviation during contingencies, but does not consider the frequency stability of the AC systems connected to the MTDC grid which can be violated in case of big disturbance. To consider this aspect, RoCoF constraint is included in our work. An adaptive multi-dimensional droop control scheme is proposed in [13] for stability enhancement of AC grids connected to MTDC power networks. The proposed adaptive multi-dimensional control scheme is designed to improve the stability of the AC frequency, voltage, and the DC voltage, but does not consider the economic part of power sharing. In [14], a distributed economic model predictive control method is proposed for economic operation and frequency regulation of the power systems interconnected through the MTDC grid. In [15] authors propose a decentralized control method based on non-linear dynamic droop control to distribute power between the super capacitor and the battery. Those energy storage systems provide primary frequency support through MTDC system using two dynamic droop gain profiles that vary nonlinearly when DC voltage changes. Although presented approach automatically splits the power between BESS and SC providing that SC is in charge of compensating the high-frequency demand, whereas the BESS is in charge of compensating the low-frequency power demand, proposed strategy does not consider constraints related to MTDC grid. A communication-free frequency regulation scheme that consists of the droop control, the inertia emulation control and the frequency safety control that enables spinning reserves sharing in hybrid AC/DC grids is proposed in [16]. Even though presented solution reduces the coupling effect among AC grids, providing that the disturbance in strong AC grids would not affect the weak AC systems, it does not provide optimal power sharing between connected AC grids. Control method that cooperatively adjust VSC-stations dc-bus voltage to change the dc power flow with the frequency deviation and load ratio based on the communication with the neighbors is presented in [17]. The proposed approach effectively utilizes the power reserves in asynchronous ac grids for restoring the frequency and achieve the balanced power dispatch during the frequency support process. Nevertheless, it does not provide optimal power dispatch based on different criteria. [2] proposed control that is based on the combination of Vdc-f droop and P-Vdc droop that enables MTDC system to work at traditional P-Vdc droop control during normal operation. Nevertheless, interaction between these two droops weakens the effectiveness of each other. Control scheme that couples inertia emulation control with nonlinear droop control is presented in [18], but authors did not consider limitation related to connecting MTDC grid.

Adaptive control of HVDC links for frequency stability enhancement is proposed in [19], where the modular multilevel converter (MMC) at the end of HVDC link provides active power support constrained only by the capacity of the MMC. The control uses only the locally measured frequency change and considers the AC system as a "black box". It consists of two stages. In the first stage, the HVDC response is triggered by locally measured RoCoF, as a disturbance indicator, and the size of the disturbance is estimated using the generator swing equation and frequency response. In the second stage, the HVDC response is adapted to the estimated size of disturbance providing more adequate support to the disturbed AC system. When the disturbance event is identified, the HVDC response in the first step is constant and equal to a predefined value. The first step of HVDC response can be determined by off-line analysis, based on an assessment of the configuration of the system and its inertia in a day ahead scheduling plan. The second step of the HVDC response removes the possibility that the initial HVDC response would be too large/small, which in the case of single-stage control must certainly happen in the event of various outages in the system. This paper is the extension of the control principles proposed in [19], with focus on how power support provided by MMC should be shared between not-affected AC systems connected to the MTDC grid.

Proposed FFR control strategies of MTDC are designed to provide frequency support rapidly and consequently, it is difficult to provide

FFR in an optimized way. To fill this research gap, we propose a FFR control strategy that enables optimal power-sharing for different criteria functions. We consider the economic aspect of power reserve sharing in terms of minimum costs, but also take into account the stability of the MTDC system by including constraints related to maximum values of RoCoF, voltages and power flow. The stability is observed through minimization of the voltage deviations while trying to ensure a limited impact on the stability of the AC systems by keeping RoCoF values in connected AC systems within defined limits. Moreover, criteria related to minimization of RoCoF values will enable high inertia AC system to take over the biggest part of active power support. Optimal droop coefficients are predefined for the list of potential disturbances in AC systems and triggered based on the location of the disturbance.

The main contribution of the presented method is that the adopted droop characteristics ensure optimal and stable operation of the MTDC grid and guaranty that no constraints are violated. The advantage of this approach is that the droop coefficients of the converters are determined offline before the potential disturbance and do not depend on the size of the disturbance. Therefore, this control strategy enables rapid response and does not dependent on telecommunication delays.

The paper is organized as follows. In Section 2, the MTDC primary controls are briefly described, together with the optimization algorithm at the secondary control level. Section 3 describes case studies for validation of the proposed control scheme and simulation results followed by discussion. Finally, some closing remarks are given in Section 4.

2. MTDC control structure

2.1. MTDC primary controls

Although there are a few different sub-module designs, the commonly used is H-bridge sub-module MMC. Therefore, in this paper we will be using H-bridge MMC model. Each MMC is controlled using various controlling loops grouped into upper and lower level controls (Fig. 1) [20].

Lower level controls of the MMC are circulating current suppression control, output current control, and voltage balancing controls for the sub-modules. Upper level control are responsible for the MMC functionality and it strongly depends on the position in the hybrid power system, i.e. onshore or offshore. For HVDC link, power controllers are used on offshore converter side to ensure satisfactory active power transfer. On offshore side is usually used active power controller together with AC voltage controller and PLL (phase locked loop) controller. If there are multiple offshore converters, then they should ensure both power sharing (i.e. active power control) as in Fig. 2b or grid forming control as depicted in Fig. 2c. DC voltage control in PI or droop form is used on onshore side to maintain DC voltage level of the HVDC transmission line, as depicted in Fig. 2a. In addition to DC voltage controller, energy controller minimizes losses inside the converter and ensures faster DC voltage and DC current convergence.

Therefore, each MMC inside the MTDC has its role and it has predefined outer control functionalities.

2.2. Optimization algorithm at the secondary control level

2.2.1. Optimal power sharing between AC systems connected to the MTDC grid

At the secondary control layer, the optimal sharing of power support between not-affected AC systems connected to the MTDC grid is calculated. To assure the minimum cost of the frequency control actions, the minimum voltage deviations, and the minimal impact on the frequencies of not-affected AC, the optimization problem is defined by the following criteria functions:

$$\min F_{cost_{FFR}} = \min \sum_{i=1,i\neq j}^{n_{AC}} c_i^{FFR}(P_i^{FFR})P_i^{FFR}, \tag{1a}$$

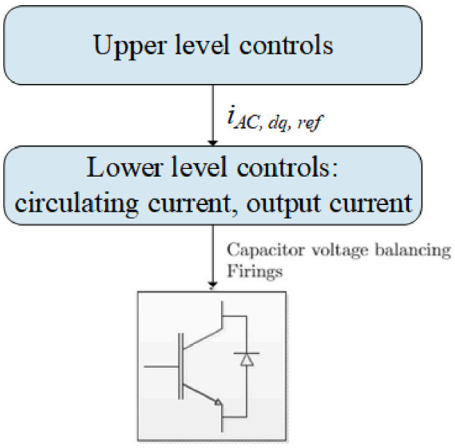

Fig. 1. High level description of control system for MMC technology.

$$\min F_{cost_U} = \min \sum_{i=1}^{n_{AC}} (U_i - U_i^{ref})^2, \tag{1b}$$

$$\min F_{RoCoF} = \min \sum_{i=1}^{n_{AC}} |RoCoF_i|, \tag{1c}$$

where P_i^{FFR} represents the FFR support from the AC system i in case of disturbance in AC system j, $c_i^{FFR}(P_i^{FFR})$ is the cost of FFR reserve in the AC system i, and n_{AC} is the number of AC systems interconnected through the MTDC grid. U_i and U_i^{ref} are DC voltage and its nominal value of the converter i, while $RoCoF_i$ is the minimum RoCoF value in the AC system i, caused by provision of the frequency support. In the following Eq. (1) the coefficients have following values: $i, j \in \{1, \ldots, n_{AC}\}$.

$RoCoF_i$ is subjected to constraint of maximum allowed RoCoF value $RoCoF_{max}$ defined as:

$$|RoCoF_i| = \left| -\frac{P_i^{FFR}}{2H_i} \right| \leq RoCoF_{max}, \quad (\forall i \neq j)(i, j \in \{1, \ldots, n_{AC}\}), \tag{2}$$

where H_i is the rotational inertia of AC system i. The emergency power allocation of converters for providing a frequency response is subjected to the constraints of the FFR reserve available in the AC systems and the capacity of connected converters:

$$P_i^{FFR} \leq P_i^{res} \quad (\forall i \neq j)(i, j \in \{1, \ldots, n_{AC}\}), \tag{3a}$$

$$P_i^{FFR} + P_i^{sch} \leq P_i^{cap} \quad (\forall i \neq j)(i, j \in \{1, \ldots, n_{AC}\}), \tag{3b}$$

$$\sum_{i=1}^{n_{AC}} P_i^{FFR} \geq P^{sp}, \tag{3c}$$

where P_i^{res} is the FFR reserve available in the AC system i, P_i^{sch} is the scheduled power transmission value on the converter i, P_i^{cap} is the capacity of converter i, and the P^{sp} is power support that the disturbed AC system needs [19]. The constrains are imposed on power flow and voltages in MTDC grid:

$$-P_{j_{max}}^{DC} \leq P_j^{DC} \leq P_{j_{max}}^{DC}, \tag{4a}$$

$$U_{i_{min}}^{DC} \leq U_i^{DC} \leq U_{i_{max}}^{DC}. \tag{4b}$$

The load flow P_j^{DC} of the DC line j should not exceed the transmission capacity limit of the DC line $P_{j_{max}}^{DC}$, as well as the voltages at the DC side of converter U_i^{DC} should not exceed defined limits $U_{i_{min}}^{DC}$ and $U_{i_{max}}^{DC}$, respectively. Power flows in DC grid can be described with equality constraint:

$$P_j^{DC} = \sum_{i=1}^{n_{DC}} U_j^{DC} U_i^{DC} G_{i,j}, \tag{5}$$

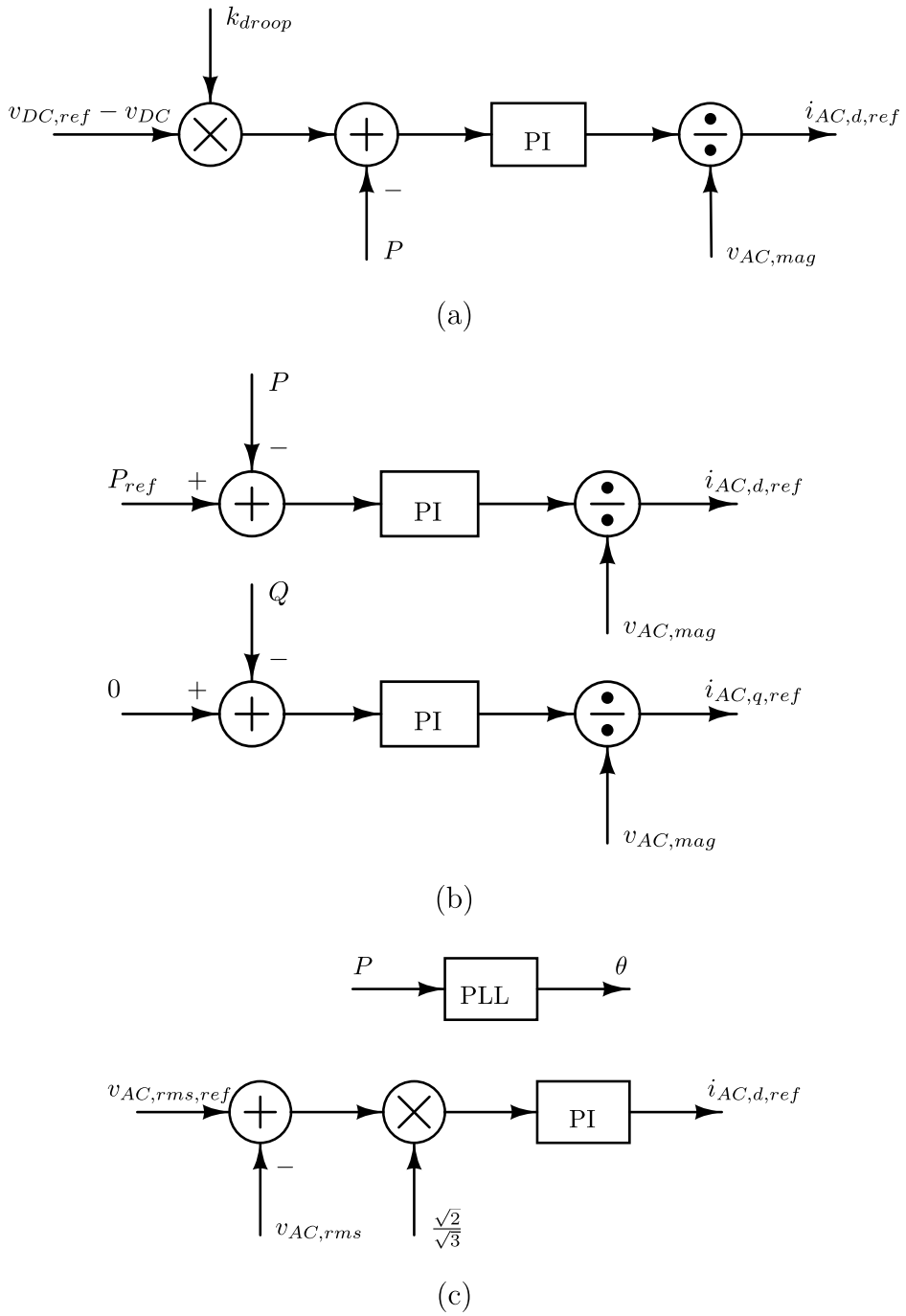

Fig. 2. Implementation of high level controllers: (a) for voltage droop-control; (b) active and reactive power control.

where $G_{i,j}$ is conductance at the position (i, j) of the network admittance matrix and n_{DC} refers to the number of lines in the DC grid. In the optimization algorithm, DC lines are modeled only as resistances since they refer to steady state values.

The change in active power of converters ΔP_i connected to the AC system i will cause the change in voltage ΔU_i at the DC side of converter $i \in \{1, \dots, n_{MMC}\}$ for n_{MMC} being the number of converters, that are connected using relation:

$$\Delta U_i = k_i \, \Delta P_i, \quad \forall i \in \{1, \dots, n_{MMC}\} \tag{6}$$

where k_i is voltage-droop characteristic of the voltage-regulating converters which should also satisfy the grid code requirements expressed as:

$$k_{min} \leq k_i \leq k_{max} \quad \forall i \tag{7}$$

where k_{min} and k_{max} represent grid code limitations for the value of the droop coefficient.

2.2.2. Obtaining the voltage-droop characteristics

The first step is to obtain the voltage-droop characteristics of the voltage-regulating converters in case of a potential disturbance in AC system connected to the grid. It can be described with following procedure:

1. Create a list of potential disturbances in the specific AC system (N_{dist} is the number of potential disturbances and $i_{current\_dist}$ is the number of the current disturbance from the defined list);
2. For an initial response of the MMC connected to disturbed AC system, obtain the optimal power sharing between not-affected AC systems connected to the MTDC grid, and consequently their DC voltages and active power references using criteria functions (1);
3. Obtain the voltage-droop characteristics of the voltage-regulating converters that contains the initial operating state and state defined in step (2);
4. Calculate the required active power support ΔP_{MMC2} delivered by the MMC for each disturbance from the defined list using the algorithm proposed in [19] as:

$$\Delta P_{MMC2} = \Delta P_{MMC1} \frac{\Delta f_1}{\Delta f_1 - \Delta f_2} RoCoF(0) \tag{8}$$

where ΔP_{MMC1} is the initial active power response of the MMC, Δf_1 is the difference between the two frequency values after the disturbance and before the MMC response, while Δf_2 is frequency deviation after the initial response of the MMC. Frequency measurements are obtained by PLL and considering that the PLL will experience frequency spikes immediately after the disturbance that can affect punctuality of obtained frequency values, the calculation of the slope of the frequency response is done on the time interval from 0.2 s to 0.5 s after the disturbance and initial MMC response. It is considered that 0.2 s after the disturbance/initial MMC response frequency transients are negligible. $RoCoF(0)$ is the initial RoCoF value which is locally measured and it is inversely proportional to system inertia. In this way, active power support is larger for the same size disturbance in a low-inertia system than in the high-inertia system, which is more adequate in terms of frequency stability. The second step of response eliminates the risk that the initial response would be too large/small, which in the case of single-stage control must certainly occur in the event of various outages in the system;
5. For calculated response, obtain the optimal power sharing between not-affected AC systems connected to the MTDC grid, and consequently their DC voltages and active power references using criteria functions (1);
6. Obtain the optimal voltage-droop characteristics of the voltage-regulating converters using least square regressions that contains the state defined in step 2.

Flowchart of the procedure to obtain optimal voltage droop characteristics is shown on Fig. 3. The output of the optimization algorithm are reference values for the voltage-droop characteristics of the voltage-regulating converters, and consequently their DC voltages and active power references. The obtained values are transferred to the primary control level where dynamical MTDC control is implemented.

3. Simulations and results

3.1. Test system

The secondary control layer is implemented in MATLAB/Simulink, while the primary is executed using RTDS. The proposed control structure is verified on a reduced model of CIGRE B4 MTDC test system (see Fig. 4) [20]. The chosen test system is denoted as DS2 in the CIGRE brochure [20].

In the MTDC there are four converters. Offshore MMC 4 and MMC 3 have an outer controlling loop for the active power control. Onshore converters MMC 1 and MMC 2 are connected to the AC grid, and they regulate active power and DC voltage using the droop controlling approach.

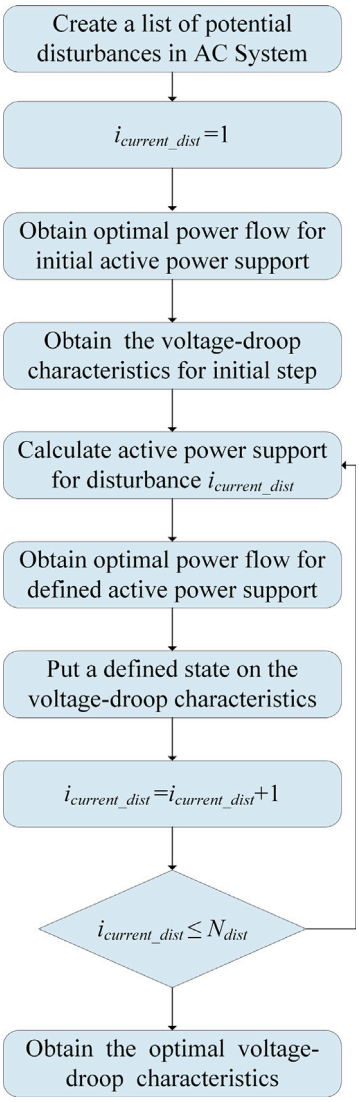

Fig. 3. Flowchart of the procedure to obtain optimal voltage droop characteristics.

Table 1
AC systems data.

	AC 1	AC 2	AC 3	AC 4
Power [GW]	4	4	4	4
Inertia [s]	5	6	5	2
FFR reserve [MW]	300	300	300	200
MMC capacity [MW]	800	1200	800	200
FFR price [€per MW]	1	2	0.5	1

Table 2
MTDC grid data.

DC line	Bus 1	Bus 1	$R[\Omega]$	Max power [MW]
l_{12}	1	2	2.22	784.8
l_{23}	2	3	2.44	784.8
l_{34}	3	4	2.22	784.8

The data of the AC systems are shown in Table 1, while the important details about MTCD grid are shown in Table 2.

The initial operating state is shown in Table 3, where the parameters of the droop characteristics are adopted based on [21], where the operating point is adjusted according to the criterion of minimum active power losses in the DC and AC grids. Fig. 5 shows the results of the proposed procedure for converter 1 and 2 in case of disturbance in

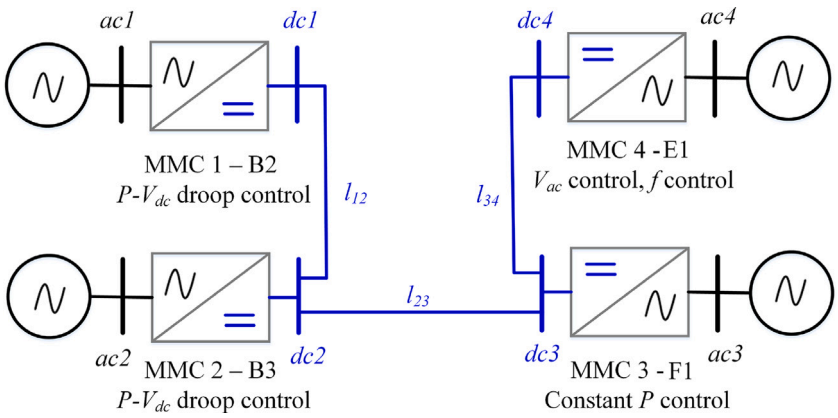

Fig. 4. MTDC power system.

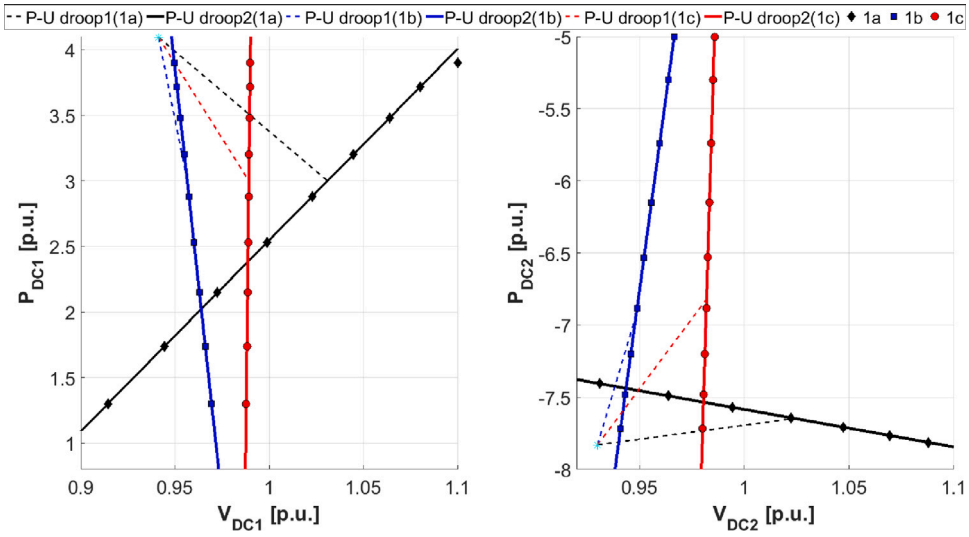

Fig. 5. Voltage-droop characteristic of converters B2 and B3 in case of a disturbance in AC system 1.

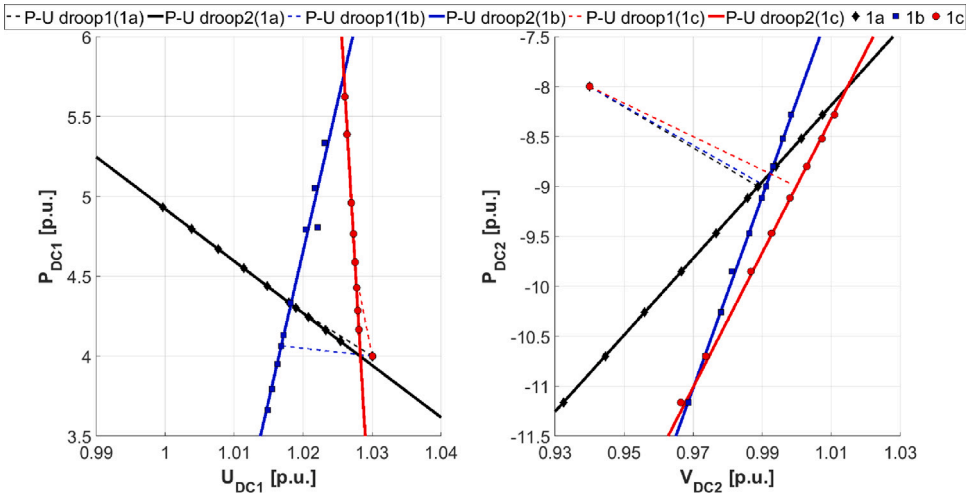

Fig. 6. Voltage-droop characteristic of converters B2 and B3 in case of a disturbance in AC system 2.

AC system 1, while Figs. 6 and 7 show the results in case of disturbance in AC system 2 and 3. Optimal values of voltage droop characteristics are presented in Table 4. The optimization problem was solved in MATLAB using *fmincon* function that finds the minimum of a constrained nonlinear multivariable function using a built-in interior-point algorithm.

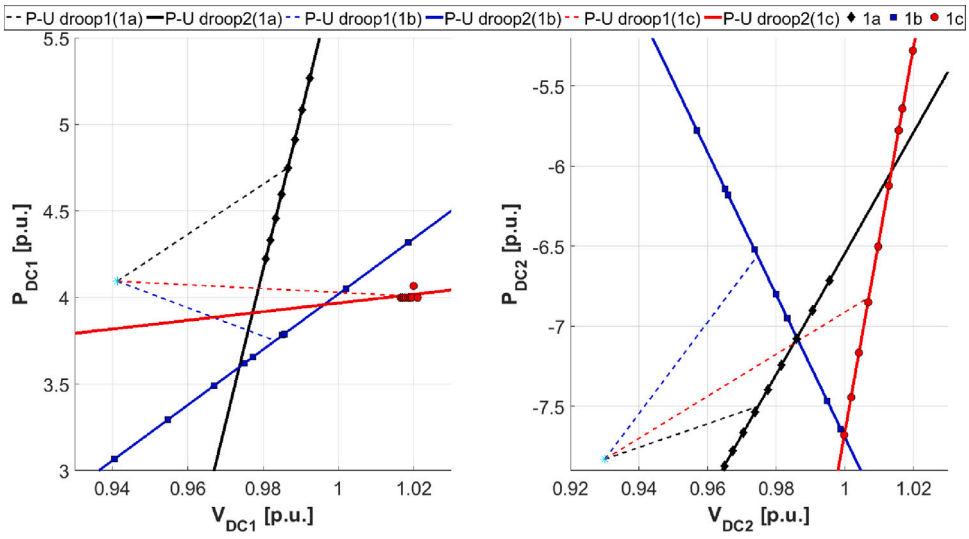

Fig. 7. Voltage-droop characteristic of converters B2 and B3 in case of a disturbance in AC system 3.

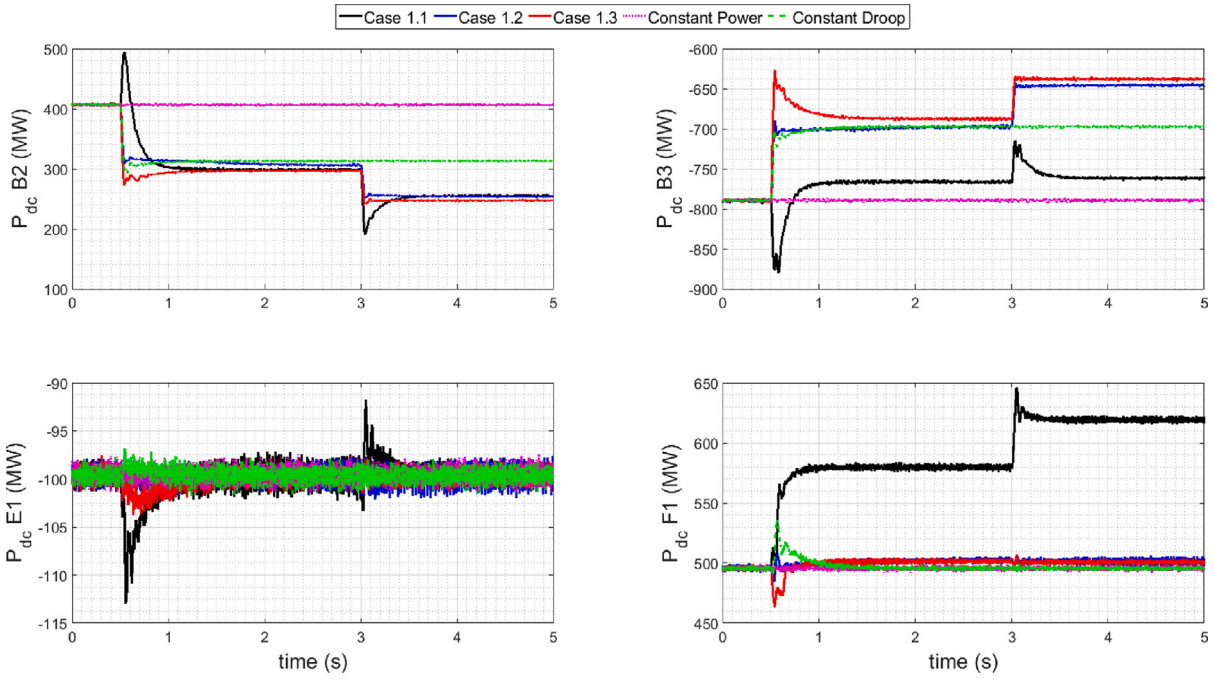

Fig. 8. Active power at the converters DC side in case of the disturbance in AC system 1.

Table 3
The initial operating state.

	dc 1	dc 2	dc 3	dc 4
U [p.u]	0.9413	0.9300	0.9416	0.9387
P_{DC} [p.u]	4.094	−7.830	5.000	−0.996
k_{droop}	0.02	0.02	–	–

The initial MMC response of 100 MW was chosen arbitrarily. For some disturbances from the list of potential disturbances, the algorithm has calculated that active power support in the second stage should be slightly less than the initial response of 100 MW. For those cases, the MTDC system will provide unnecessary active power support in the initial step and then adjust the response to a smaller value in the second step. This situation could have been avoided by choosing a step that was lower than calculated active power support for the smallest disturbance. On the other hand, the larger size of the initial step is favorable for the estimation of the disturbance size, since it is closer to the actual disturbance (i.e. the estimation error is smaller). On the other hand, in the case of larger disturbances, when the calculated support by MTDC is higher, having a larger initial step will allow reaching the operating point faster, which is of great importance in the case of critical disturbances.

3.2. Simulations

We studied two scenarios:

- Scenario 1: A generator outage in AC system 1 equal to 500 MW;
- Scenario 2: A generator outage in AC system 3 equal to 500 MW.

For each scenario, three case studies were considered:

- Case 1 – Criteria function 1a;

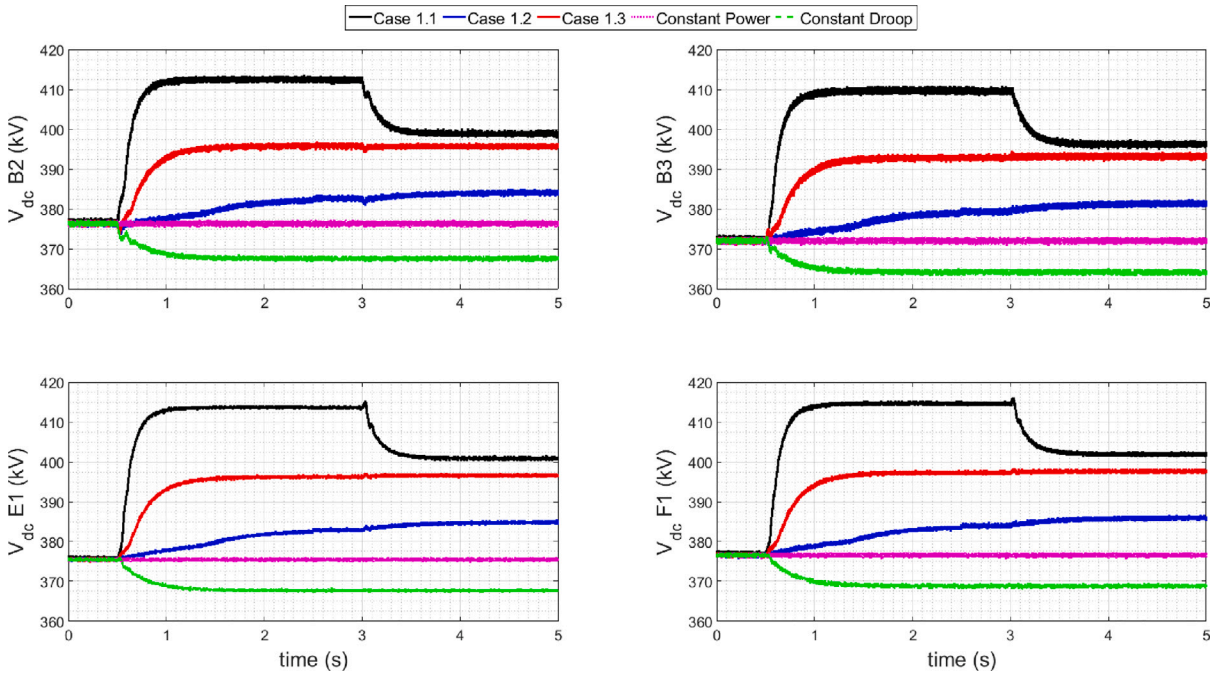

Fig. 9. Voltage at the converters DC side in case of the disturbance in AC system 1.

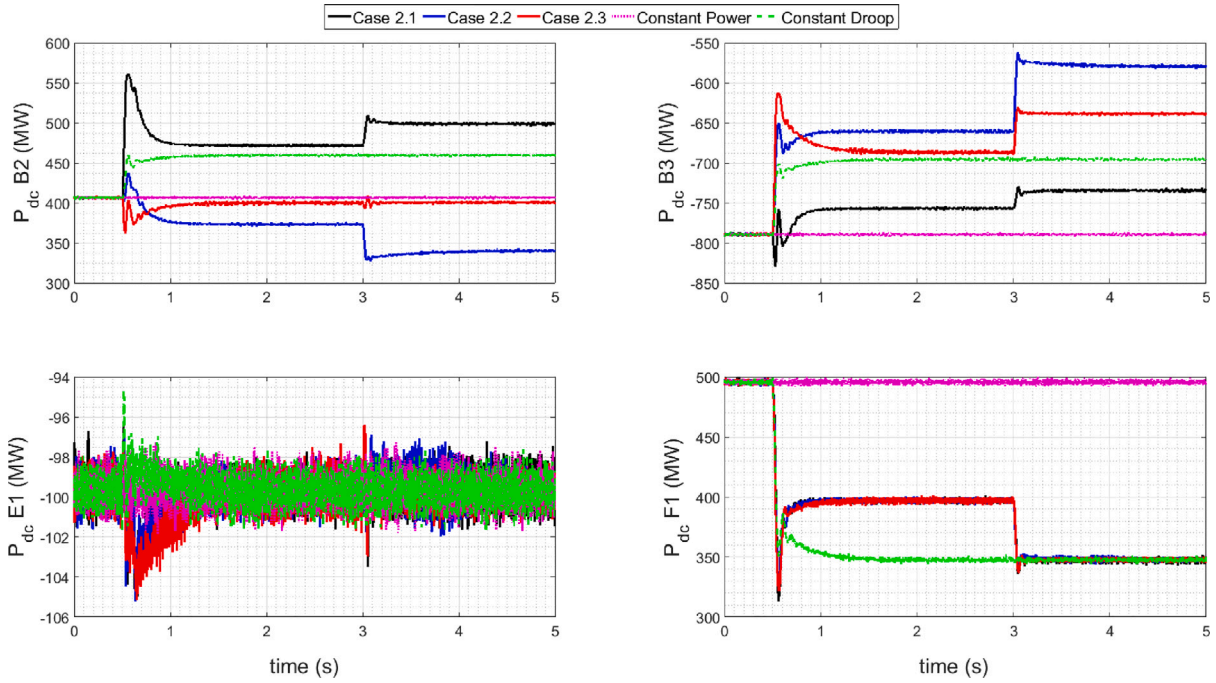

Fig. 10. Active power at the converters DC side in case of the disturbance in AC system 3.

- Case 2 – Criteria function 1b;
- Case 3 – Criteria function 1c.

All simulations are performed using state-of-the-art electromagnetic transient (EMT) simulation tool RSCAD/RTDS.

Active powers at the converters DC side in case of the disturbance in AC system 1 are presented in Fig. 8, while the voltages are given in Fig. 9. To compare performance, results for constant power control and conventional droop control are also presented. In Scenario 1, for all case studies, the change of active power at the converter B3, which connects AC system 1 to the MTDC network, is the same regardless of the choice of criterion function. This is because the active power support to the AC system in which the disturbance occurred is defined according to the algorithm shown in [19]. The active power change on other converters depends on the criterion function and it is different for different case studies. For case study 1.1 where the criterion function minimizes reserve costs, the largest contribution is from the AC3 system which is connected to the MTDC network via converter E1 because the reserve price of that system is the least expensive (Table 1). In the case of conventional droop control, the active power support needed for AC1 should be the same as in previous cases, but it was not delivered totally since the constant droop control could not provide that active power change at converter B2. In the case of constant power control AC

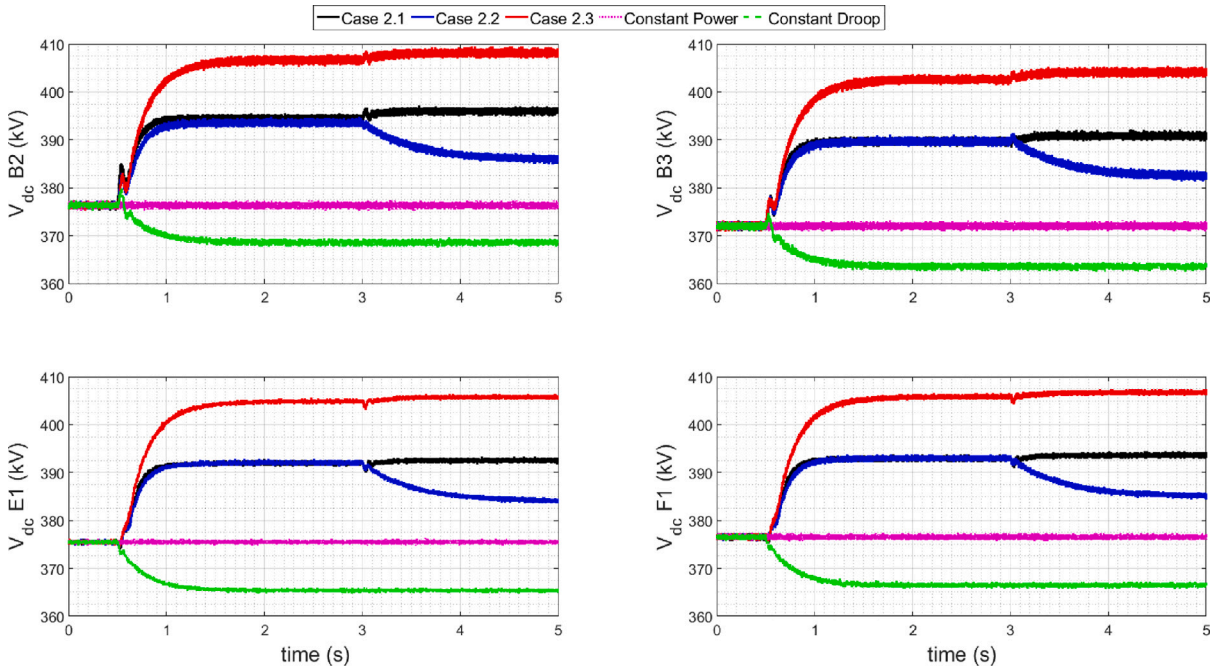

Fig. 11. Voltage at the converters DC side in case of the disturbance in AC system 3.

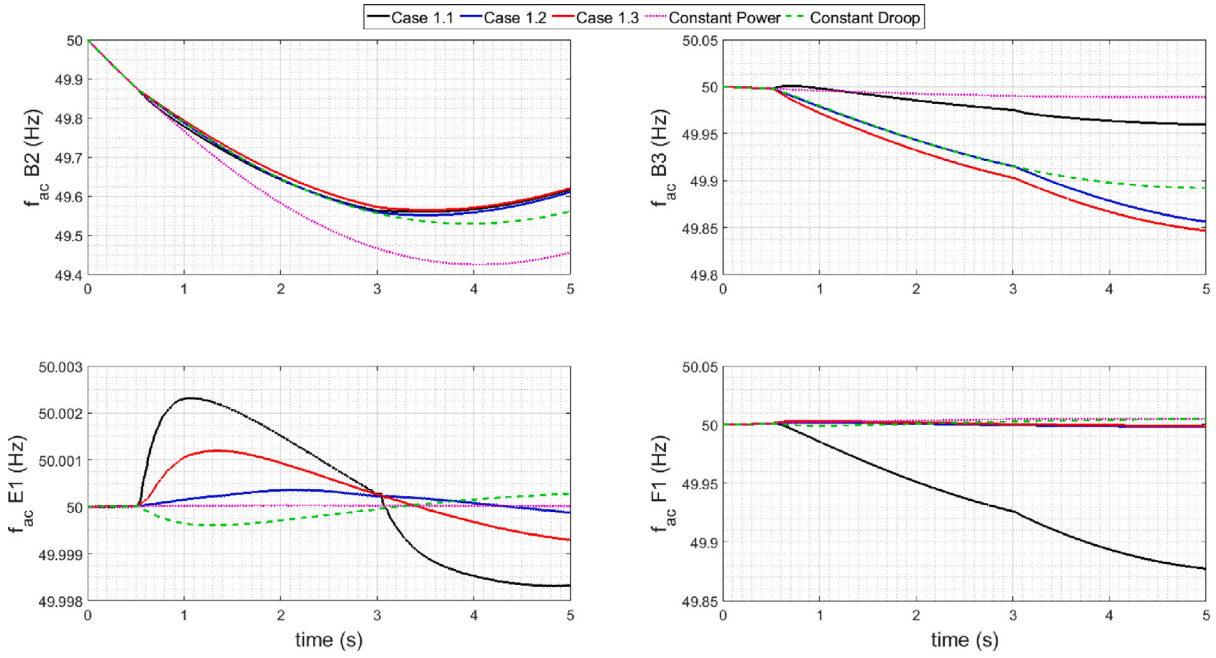

Fig. 12. Frequency in AC systems connected to the MTDC grid in case of the disturbance in AC system 1.

systems 2, 3 and 4 will not provide frequency support for AC system 1 after a disturbance, and active powers at the converters' DC side will remain the same.

In the study case 1.3, where the criterion function minimizes RoCoF values, it can be seen that the largest contribution is from the AC2 system which is connected to the MTDC network via converter B3. AC2 system has the biggest inertia comparing to other AC systems and the power change will lead to the smallest RoCoF deviation. On the other hand, when we look at case study 1.2 where the voltage deviations are minimized (see Fig. 9), it can be seen that the voltage changes are the smallest.

In the scenario 2, when the disturbance was in AC system 3, the observations are similar to those in scenario 1 for the defined criterion functions. Active power and voltages at the converters DC side in case of the disturbance in AC3 are presented in Figs. 10 and 11. As for the frequency behavior and RoCof in the systems, they are shown in Figs. 12 and 13 for Scenario 1, and in Figs. 14 and 15 for Scenario 2. In the case of constant power control, the frequency will have the lowest value in the system where disturbance happened and can activate the under-frequency load shedding which can result in a wide-area blackout in the disturbed system. When the conventional droop control scheme is adopted, the frequency is below the values compared to cases with the proposed control. Moreover, in the case of a conventional droop control scheme, the active power support sharing between AC systems is not optimal and does not consider the constraints of the available reserve as well as the limitations of the DC grid. It can be

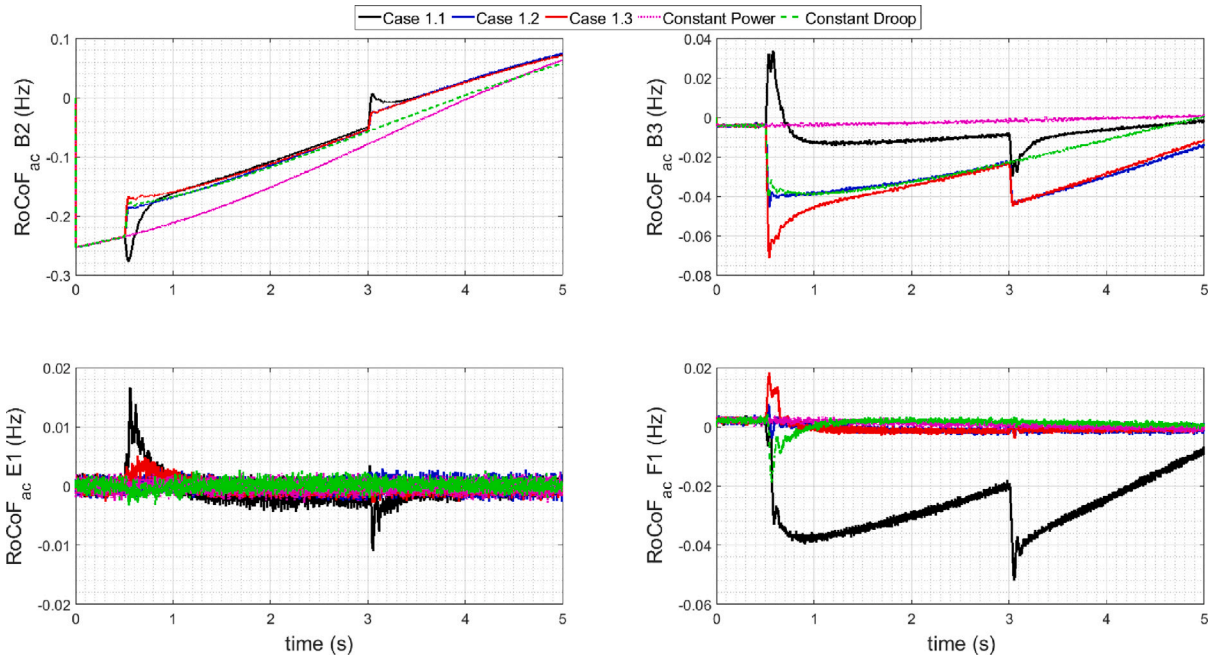

Fig. 13. RoCoF in AC systems connected to the MTDC grid in case of the disturbance in AC system 1.

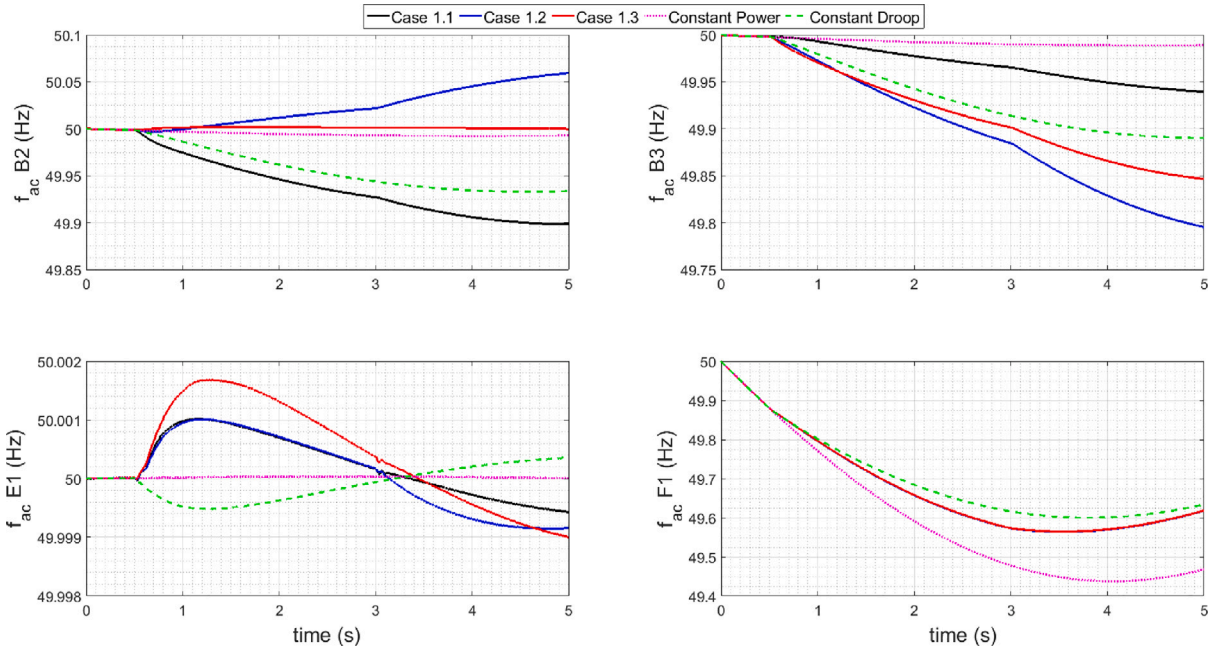

Fig. 14. Frequency in AC systems connected to the MTDC grid in case of the disturbance in AC system 3.

Table 4
The optimal voltage droop characteristics.

	Criteria 1a		Criteria 1b		Criteria 1c	
Disturbance in AC system 1						
k_1	−1.5245	1.8222	−8.9967	−16.4474	−2.8549	15.6250
k_2	0.2434	−0.3246	6.1141	13.2653	2.4279	16.6215
Disturbance in AC system 2						
k_1	−1.2513	−1.1256	−0.4167	18.4587	−17.2485	−23.5472
k_2	−3.1254	12.5	−3.0954	18.4567	−2.9450	15.5894
Disturbance in AC system 3						
k_1	1.8102	11.1607	−1.0263	8.0214	−0.1387	0.3125
k_2	0.9228	4.7170	3.5674	−5.5556	1.6396	15.0000

seen in Figs. 9 and 11 that the voltages, in that case, are below 0.95 p.u. Performance assessment showed the dominance of proposed control for all criteria functions. Quantities comparisons are presented in Tables 5 and 6.

4. Conclusion

This paper proposes a two-layer control structure of the MTDC system which provide active power support to connected AC systems in case of a frequency disturbance. The droop control is adopted due to its distributed nature and non-complex implementation. Power-sharing between non-affected AC systems connected to the MTDC grid is determined by the droop settings of the converters. The realization of control objectives relies on the secondary control layer which is

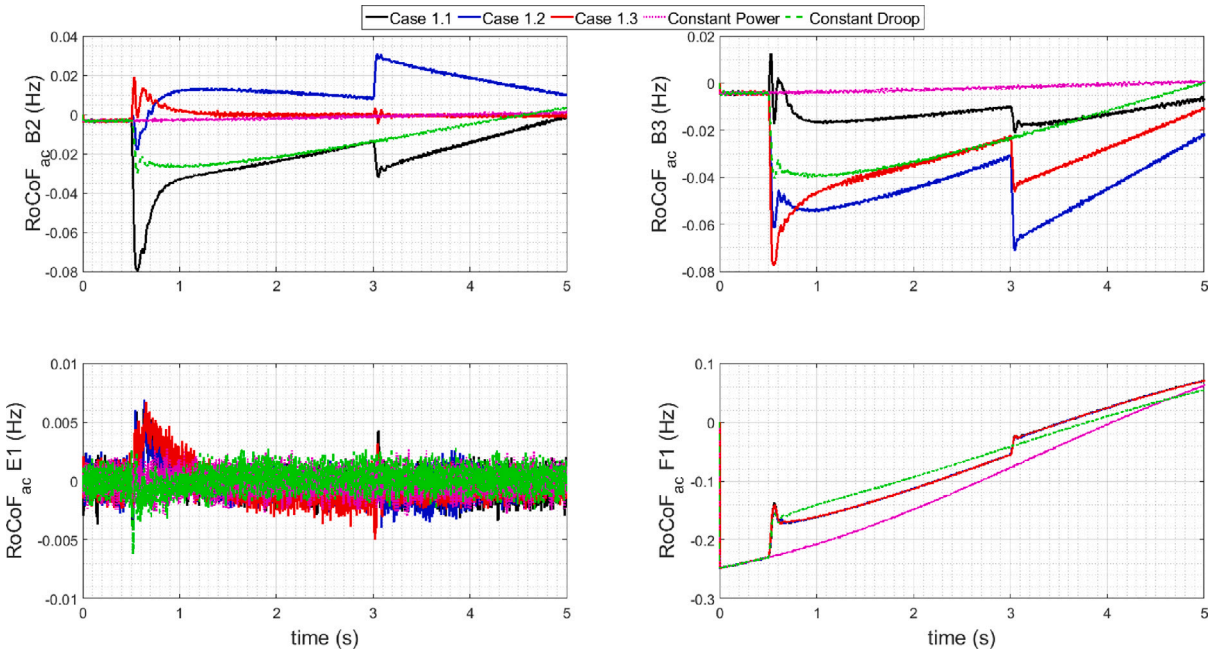

Fig. 15. RoCoF in AC systems connected to the MTDC grid in case of the disturbance in AC system 3.

Table 5
Quantities comparison in case of disturbance in AC system 1.

		Case 1.1	Case 1.2	Case 1.3	Constant power	Constant droop
P_{DC}(MW)	B2	255.3	255.7	247.4	407.9	313.2
	B3	−761.6	−645.6	−636.6	−791.0	−760.9
	E1	−97.1	−97.6	−98.6	−98.5	−99.0
	F1	617.1	504.2	501.8	500.1	499.8
V_{DC}(kV)	B2	399.4	384.7	395.9	376.6	367.4
	B3	396.6	382.2	393.1	372.5	364.5
	E1	401.1	385.0	396.3	374.8	368.1
	F1	401.6	385.1	397.4	377.2	369.3
f_{AC}(Hz)	B2	49.56	49.55	49.55	49.53	49.43
	B3	49.96	49.86	49.85	49.99	49.89
	E1	50	50	50	50	50
	F1	49.88	50	50	50	50
Criteria	1a	255.45	431.60	455.70	–	372.10
	1b	2408.0	333.15	1685.2	–	547.76
	1c	46.7500	46.1800	42.6417	–	51.0517

Table 6
Quantities comparison in case of disturbance in AC system 3.

		Case 1.1	Case 1.2	Case 1.3	Constant power	Constant droop
P_{DC}(MW)	B2	499.6	340.5	405.2	407.9	459.9
	B3	−735.7	−577.8	−638.2	−790.3	−732.8
	E1	−99.6	−98.6	−99.6	−97.5	−98.0
	F1	350.1	350.0	350.2	500.1	350.1
V_{DC}(kV)	B2	396.3	386.1	408.4	376.6	369.0
	B3	390.3	383.4	404.5	372.1	363.9
	E1	392.5	384.2	406.4	375.9	365.6
	F1	393.9	385.5	406.6	376.6	366.2
f_{AC}(Hz)	B2	49.90	50.06	50	50	49.93
	B3	49.94	49.8	49.85	50	49.89
	E1	50	50	50	50	50
	F1	49.57	49.57	49.57	49.44	49.60
Criteria	1a	259.8	555.3	368.8	–	387.5
	1b	1313.7	376.27	3926.2	–	498.76
	1c	45.6347	42.2347	40.7857	–	49.3475

implemented offline. The paper considers criteria functions that include an economic aspect of frequency regulation, MTDC stability, and the frequency stability of AC systems. The output of the secondary control layer is optimal droop characteristics of voltage regulating converters that are forwarded to the primary control layer. The performance of the proposed controller is successfully evaluated through real-time

simulation in RSCAD/RTDS and results confirm that the MTDC can provide active power support to disturbed AC systems without endangering its stability.

CRediT authorship contribution statement

Jelena Stojković: Conceptualization, Methodology, Software, Validation, Writing – original draft, Writing – review & editing. **Ajay Shetgaonkar:** Software, Validation, Visualization. **Predrag Stefanov:** Conceptualization, Methodology, Supervision. **Aleksandra Lekić:** Writing – review & editing, Conceptualization, Methodology, Supervision.

Declaration of competing interest

The authors declare that they have no known competing financial interests or personal relationships that could have appeared to influence the work reported in this paper.

Data availability

Data will be made available on request.

Acknowledgments

This project has been partially supported by the Dutch Ministry of Education, Culture and Science (OCW) through the Sector Plan Committee for Science and Technology project granted to the Technical University of Delft.

Appendix. Stability elaboration

For the MTDC control structure described in Section 2, the differential equation for the frequency can be written in the matrix format:

$$2f_0\,\mathbf{H}\,\Delta\dot{\mathbf{f}} = -\Delta\mathbf{P}, \tag{A.1}$$

for N_{ac} being the number of AC connections, vectors $\Delta\mathbf{f} = [f_1, f_2, \ldots, f_{N_{ac}}]^T$ and $\Delta\mathbf{P} = [P_1, P_2, \ldots, P_{N_{ac}}]^T$, and matrix $\mathbf{H} = \mathrm{diag}\{H_1, H_2, \ldots, H_{N_{ac}}\}$.

To depict the stability of this system, it is necessary to define Lyapunov function:

$$V(\Delta\mathbf{f}) = \frac{1}{2}\Delta\mathbf{f}^T\,\mathbf{P}\,\Delta\mathbf{f} \tag{A.2}$$

with $\mathbf{P} \succ 0$ being the positive definite matrix. The system is stable when the time derivative of the corresponding Lyapunov function is negative. Let us first assume that the matrix $\mathbf{P}$ is an identity matrix with the size $N_{ac} \times N_{ac}$. Then,

$$\dot{V}(\Delta\mathbf{f}) = \frac{1}{2}\Delta\mathbf{f}^T\,(\mathbf{A}^T\,\mathbf{P} + \mathbf{P}\,\mathbf{A})\,\Delta\mathbf{f} + \Delta\mathbf{f}^T\,\mathbf{P}\,\mathbf{B}. \tag{A.3}$$

From Eq. (A.1) is obvious that matrix $\mathbf{A}$ is zero matrix, since there is no right hand side part in the differential equation that represents multiple of $\Delta\mathbf{f}$. Furthermore, one might see that $\mathbf{B} = -\Delta\mathbf{P}$. Thus, we can write

$$\dot{V}(\Delta\mathbf{f}) = -\Delta\mathbf{f}^T\,\Delta\mathbf{P}. \tag{A.4}$$

In case when the change of the droop characteristics occurs (vectors denoted as $\mathbf{k^1}$ and $\mathbf{k^2}$), then we define Lyapunov function using Eq. (A.2) for both operating regions, denoted with subscripts 1 and 2. For the complete stability of the system according to Filippov [22], it is necessary to check the behavior of the system on the switching hyperplanes where the Lyapunov function derivative does not exist. In order to do that, we have to show that on these hyperplanes the following differential inclusion inequality is satisfied for $\alpha, \beta \in [0, 1]$:

$$(\beta\,\mathrm{grad}\,V(\Delta\mathbf{f})|_1) + (1-\beta)\,\mathrm{grad}\,V(\Delta\mathbf{f})|_2\,(\alpha\Delta\dot{\mathbf{f}}|_1 + (1-\alpha)\,\Delta\dot{\mathbf{f}}|_2) < 0. \tag{A.5}$$

This condition should be checked at each intersection of hyperplanes defined with droop coefficients in the vector representation $\mathbf{k}$.

References

[1] Milano F, Dörfler F, Hug G, Hill DJ, Verbič G. Foundations and challenges of low-inertia systems. In: 2018 Power systems computation conference. IEEE; 2018, p. 1–25.
[2] Adeuyi OD, Cheah-Mane M, Liang J, Jenkins N. Fast frequency response from offshore multiterminal VSC–HVDC schemes. IEEE Trans Power Deliv 2016;32(6):2442–52.
[3] Orellana L, Matilla V, Wang S, Adeuyi OD, Ugalde-Loo CE. Fast frequency support control in the GB power system using VSC-HVDC technology. In: 2017 IEEE PES Innovative smart grid technologies conference Europe (ISGT-Europe). IEEE; 2017, p. 1–6.
[4] Dai J, Phulpin Y, Sarlette A, Ernst D. Coordinated primary frequency control among non-synchronous systems connected by a multi-terminal high-voltage direct current grid. IET Gener Transm Distribut 2012;6(2):99–108.
[5] Vrana TK, Beerten J, Belmans R, Fosso OB. A classification of DC node voltage control methods for HVDC grids. Electr Power Syst Res 2013;103:137–44.
[6] Wang R, Chen L, Zheng T, Mei S. VSG-based adaptive droop control for frequency and active power regulation in the MTDC system. CSEE J Power Energy Syst 2017;3(3):260–8.
[7] Li Y, Liu S, Zhu J, Yuan X, Xu Z, Jia K. Novel MTDC droop scheme with decoupled power control for enhancing frequency stabilities of weak AC systems. IET Renew Power Gener 2020;14(11):2007–16.
[8] Andreasson M, Wiget R, Dimarogonas DV, Johansson KH, Andersson G. Distributed frequency control through MTDC transmission systems. IEEE Trans Power Syst 2016;32(1):250–60.
[9] Song S, McCann RA, Jang G. Cost-based adaptive droop control strategy for VSC-MTDC system. IEEE Trans Power Syst 2020;36(1):659–69.
[10] Wang Y, Wen W, Wang C, Liu H, Zhan X, Xiao X. Adaptive voltage droop method of multiterminal VSC-HVDC systems for DC voltage deviation and power sharing. IEEE Trans Power Deliv 2018;34(1):169–76.
[11] Nguyen VTK, Wu Y-K, Phan QD. Adaptive droop control for compromise between DC voltage and frequency in multi-terminal HVDC. IEEE Access 2021.
[12] Satish Kumar A, Prasad Padhy B. Adaptive droop control strategy for autonomous power sharing and DC voltage control in wind farm-MTDC grids. IET Renew Power Gener 2019;13(16):3180–90.
[13] Gu M, Meegahapola L, Wong KL. Coordinated voltage and frequency control in hybrid AC/MT-HVDC power grids for stability improvement. IEEE Trans Power Syst 2020;36(1):635–47.
[14] Jia Y, Meng K, Sun C, Yuan L, Dong ZY. Economic-driven frequency regulation in multi-terminal HVDC systems: A cooperative distributed approach. IEEE Trans Power Syst 2019;35(3):2245–55.
[15] Shadabi H, Kamwa I. A decentralized non-linear dynamic droop control of a hybrid energy storage system bluefor primary frequency control in integrated AC-MTDC systems. Int J Electr Power Energy Syst 2022;136:107630.
[16] Xiao H, Sun K, Pan J, Xiao L, Gan C, Liu Y. Coordinated frequency regulation among asynchronous AC grids with an MTDC system. Int J Electr Power Energy Syst 2021;126:106604.
[17] Wang W, Yin X, Cao Y, Jiang L, Li Y. A distributed cooperative control based on consensus protocol for VSC-MTDC systems. IEEE Trans Power Syst 2021;36(4):2877–90.
[18] Liu B, Chen Z, Yang S, Wang Y, Yang K, Lu C. Primary frequency regulation scheme applicable to LCC–VSC series hybrid HVDC considering AC voltage stability at receiving end. Int J Electr Power Energy Syst 2022;140:108071.
[19] Stojković J, Lekić A, Stefanov P. Adaptive control of HVDC links for frequency stability enhancement in low-inertia systems. Energies 2020;13(23):6162.
[20] Vrana TK, Yang Y, Jovcic D, Dennetière S, Jardini J, Saad H. The CIGRE B4 DC grid test system. Electra 2013;270(1):10–9.
[21] Kotur D, Stefanov P. Optimal power flow control in the system with offshore wind power plants connected to the MTDC network. Int J Electr Power Energy Syst 2019;105:142–50.
[22] Filippov AF. Differential equations with discontinuous righthand sides: control systems, vol. 18. Springer Science & Business Media; 2013.